A Model Compound of Novel Cofactor Tryptophan Tryptophylquinone of Bacterial Methylamine Dehydrogenases. Synthesis and Physicochemical Properties

Shinobu Itoh,*,† Masaki Ogino,† Shigenobu Haranou,† Tadashi Terasaka,† Takeya Ando,† Mitsuo Komatsu,† Yoshiki Ohshiro,† Shunichi Fukuzumi,*,† Kenji Kano,‡ Kazuyoshi Takagi,‡ and Tokuji Ikeda‡

Contribution from the Department of Applied Chemistry, Faculty of Engineering, Osaka University, 2-1 Yamada-oka, Suita, Osaka 565, Japan, and Department of Agricultural Chemistry, Faculty of Agriculture, Kyoto University, Sakyo, Kyoto 606, Japan

Received August 22, 1994[⊗]

Abstract: The synthesis and physicochemical characterization of the model compound (**1**) of novel cofactor TTQ (tryptophan tryptophylquinone), the active center of bacterial methylamine dehydrogenases (MADH), are described. The synthesis of compound **1** [3-methyl-4-(3′-methylindol-2′-yl)indole-6,7-dione] has been accomplished by starting with 2-carbomethoxy-3-methyl-7-methoxyindole (**2**) as follows. Friedel−Crafts acylation on **2** with propionyl chloride gave the 4-acylated compound, which was converted into 3-methyl-4-propionyl-7-methoxyindole (**5**) by ester hydrolysis followed by thermal decarboxylation. Construction of the second indole ring by Fischer indolization with phenylhydrazine hydrochloride, followed by deprotection of the methoxy group, gave 7-hydroxy derivative **7**, which was finally converted into model compound **1** by oxidation with Fremy's salt. Another simple pathway mimicking one of the postulated biosynthetic routes was also investigated; hydroxyskatoles were oxidized into a 6,7-indolequinone derivative and then coupled with skatole itself using $AlCl_3$ as a catalyst to give **1**. Strong resemblances in several spectroscopic properties and in molecular geometry exist between **1** and TTQ cofactor in MADH. Compound **1** exhibits a pair of reversible waves ascribed to a two-electron redox reaction of the quinoid moiety. At pH 7.0, the formal potential *vs* NHE is 0.107 V, which is close to that of the native enzyme (0.126 V). The spectroscopic titration and the formal potential measurements were employed to determine the pK_a values of **1** (10.6−10.9) and its reduced form $\mathbf{1H_2}$ (10.1). Detailed digital simulation analysis of the voltammograms has revealed a two-step one-electron transfer mechanism *via* its semiquinone radical ($\mathbf{1}^{\bullet-}$), allowing for the evaluation of the two one-electron redox potentials. The EPR spectroscopic measurements suggest a partial π-conjugation between the two indole rings and a nonrigid conformation. Reaction of **1** with free ammonia leads to iminoquinone **13**, which is reduced electrochemically at a more positive electrode potential than **1**. The thermodynamics and kinetics of the iminoquinone formation are also reported in detail. Generation of a radical species derived from **13** and its stability in comparison with $\mathbf{1}^{\bullet-}$ were also examined electrochemically and by EPR measurements.

Introduction

TTQ (tryptophan tryptophylquinone) is a novel cofactor that was found in bacterial methylamine dehydrogenases (MADH, EC 1.4.99.3) in 1991.[1,2] It has a unique heterocyclic *o*-quinone skeleton of 6,7-indolequinone with a 2-indolyl group at the 4-position. This cofactor is the redox center of MADH that catalyzes the oxidation of methylamine to formaldehyde and ammonia and donates two electrons to a blue copper protein, amicyanin (eq 1).[3] For the enzymatic amine-oxidation reaction,

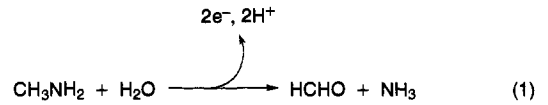

(1)

a *transamination mechanism* has been proposed,[1,4,5] and that was recently confirmed by an EPR study showing that the substrate amine nitrogen is incorporated into the substrate-reduced cofactor.[6] Very little is known, however, about the chemistry of TTQ at a molecular level.

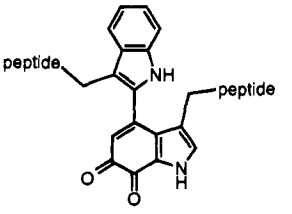

TTQ

TTQ is derived from two tryptophan residues of the MADH subunit peptide chain *via* posttranslational modification.[7] TTQ

† Osaka University.
‡ Kyoto University.
⊗ Abstract published in *Advance ACS Abstracts,* January 15, 1995.

(1) McIntire, W. S.; Wemmer, D. E.; Chistoserdov, A.; Lidstrom, M. E. *Science* **1991**, *252*, 817.

(2) (a) Chen, L.; Mathews, F. S.; Davidson, V. L.; Huizinga, E. G.; Vellieux, F. M. D.; Duine, J. A.; Hol, W. G. J. *FEBS Lett.* **1991**, *287*, 163. (b) Chen, L.; Mathews, F. S.; Davidson, V. L.; Huizinga, E. G.; Vellieux, F. M. D.; Hol, W. G. J. *Proteins* **1992**, *14*, 288.

(3) (a) Chen, L.; Durley, R.; Poliks, B. J.; Hamada, K.; Chen, Z.; Mathews, F. S.; Davidson, V. L.; Satow, Y.; Huizinga, E.; Vellieux, F. M. D.; Hol, W. G. J. *Biochemistry* **1992**, *31*, 4959. (b) Chen, L.; Mathews, F. S.; Davidson, V. L.; Tegoni, M.; Rivetti, C.; Rossi, G. L. *Protein Sci.* **1993**, *2*, 147. (c) Chen, L.; Durley, R. C. E.; Mathews, F. S.; Davidson, V. L. *Science* **1994**, *264*, 86.

(4) Backes, G.; Davidson, V. L.; Huitema, F.; Duine, J. A.; Sanders-Loehr, J. *Biochemistry* **1991**, *30*, 9201.

(5) (a) Davidson, V. L.; Jones, L. H.; Graichen, M. E. *Biochemistry* **1992**, *31*, 3385. (b) Davidson, V. L.; Jones, L. H. *Biochim. Biophys. Acta* **1992**, *1121*, 104. (c) Brooks, H. B.; Jones, L. H.; Davidson, V. L. *Biochemistry* **1993**, *32*, 2725.

(6) Wamcke, K.; Brooks, H. B.; Babcock, G. T.; Davidson, V. L.; McCracken, J. *J. Am. Chem. Soc.* **1993**, *115*, 6464.

0002-7863/95/1517-1485$09.00/0

is thus tightly associated in the enzyme matrix through an amide linkage, making it very difficult to isolate the cofactor intact and to perform mechanistic studies on the redox reactions of TTQ itself in detail. Under such circumstances, the synthesis of a model compound and a study on the chemical properties would be a breakthrough to elucidate the structure as well as the function of the TTQ cofactor. We report herein the first successful synthesis of a TTQ model compound as well as the spectroscopic and physicochemical characteristics. These results provide valuable insight into the structure and property of TTQ cofactor in the active site of MADH.[8]

Experimental Section

The chemicals used in this study were purified by the standard methods, if necessary.[9] Melting points were determined with a Yamato MP-21 apparatus and are uncorrected. IR spectra were recorded with a Hitachi 270-30 spectrophotometer and UV−vis spectra with a Shimadzu UV-265 spectrophotometer equipped with a Shimadzu TCC-260 thermostated cell holder. Mass spectra were recorded with a JEOL JNX-DX303 HF mass spectrometer or a Shimadzu GCMS-QP2000 gas chromatograph mass spectrometer. ^{1}H NMR and ^{13}C NMR spectra were recorded on a JEOL FT-NMR EX-270 spectrometer. Electron paramagnetic resonance (EPR) spectra were recorded on a JEOL JES-RE2X spectrometer with a quartz flat cell. The g values and hyperfine splitting (hfs) constants were calibrated by using an Mn^{2+} marker. The magnitude of modulation was chosen to optimize the resolution and the signal-to-noise (S/N) ratio of the observed spectra. The simulations of EPR spectra were performed by using an NEC PC-9801 RA microcomputer. The resonance Raman spectrum was obtained on a JASCO R-800 by using 457.9 nm excitation (100 mW) (KBr disk sample).

The cyclic voltammetry measurements were performed on a Yanagimoto P-1100 potentiostat controlled with an NEC PC-9801 RA microcomputer[10] with a three-electrode system consisting of a glassy carbon working electrode with ϕ = 3.0 mm (Bioanalytical System or Yanagimoto), a platinum plate auxiliary electrode, and an Ag/AgCl (saturated KCl) reference electrode. The glassy carbon electrode was polished with 0.05 μm alumina powder, sonicated to remove it, and washed with water. All electrochemical measurements were carried out at 25 °C under an atmospheric pressure of nitrogen, which was previously passed through a solution of the same composition as the electrolysis solution. An aliquot (2−20 μL) of a stock solution of **1** (*ca.* 10^{-2} M) in DMSO was injected into 1.0 mL of electrolysis solutions. Current−potential curves were theoretically analyzed by normal explicit finite difference digital simulation coupled with a nonlinear least-squares method. Details of the procedure have been described elsewhere.[11] All pH values of aqueous/organic mixed solvents were measured with a conventional pH meter and indicated without correction.

Molecular orbital calculations were performed with the MOPAC program (Version 6) by using a CAChe Work System (SONY Tektronix) and a MOL-GRAPH program (Version 2.8) (Daikin Industries, Ltd.).[12] Final geometries and energetics were obtained by optimizing the total molecular energy with respect to all structural variables.

2-Carbomethoxy-3-methyl-4-propionyl-7-methoxyindole (3). 2-Carbomethoxy-3-methyl-7-methoxyindole (**2**) was prepared according to the reported procedure.[13] Propionyl chloride (7.5 mmol) was added into a CS_2 (40 mL) solution of **2** (525 mg, 2.4 mmol) and $AlCl_3$ (640 mg, 4.8 mmol), and the mixture was stirred at refluxing temperature for 4 h. After removal of the solvent, the resulting residue was extracted with ether and dried over $MgSO_4$. Removal of the solvent gave a crude product that was purified by flash column chromatography (SiO_2, $CHCl_3$) (93% yield): mp 151−153 °C; IR (KBr) 3356 (NH), 1692 and 1672 cm^{-1} (C=O); ^{1}H NMR ($CDCl_3$) δ 1.26 (3 H, t, J = 7.3 Hz, CH_2CH_3), 2.58 (3 H, s, 3-CH_3), 3.00 (2 H, q, J = 7.3 Hz, CH_2CH_3), 3.95 (3 H, s, $COOCH_3$), 4.00 (3 H, s, 7-OCH_3), 6.66 (1 H, d, J = 7.8 Hz, 6-H, about 18% NOE was detected when irradiated at 7-OCH_3), 7.38 (1 H, d, J = 7.8 Hz, 5-H), 9.04 (1 H, br s, NH); MS (EI) m/z 275 (M^+). Anal. Calcd for $C_{15}H_{17}NO_4$: C, 65.43; H, 6.23; N, 5.09. Found: C, 65.25; H, 6.22; N, 5.07.

2-Carboxy-3-methyl-4-propionyl-7-methoxyindole (4). The indole derivative **3** (40 mg, 0.15 mmol) was treated with KOH (2 mmol) in CH_3CN−H_2O (1:1, 4 mL) at 80 °C for 1 h. Acidification of the reaction mixture with 1 N HCl gave a white precipitate that was isolated by centrifugation and dried *in vacuo* (79%): mp 226−228 °C; IR (KBr) 3492 (NH), 1682 and 1662 cm^{-1} (C=O); ^{1}H NMR ($CDCl_3$) δ 1.27 (3 H, t, J = 7.6 Hz, CH_2CH_3), 2.63 (3 H, s, 3-CH_3), 3.02 (2 H, q, J = 7.6 Hz, CH_2CH_3), 4.02 (3 H, s, 7-OCH_3), 4.1 (1 H, br, COOH), 6.69 (1 H, d, J = 8.4 Hz, 6-H), 7.40 (1 H, d, J = 8.4 Hz, 5-H), 9.10 (1 H, br s, NH); MS (EI) m/z 261 (M^+). The high-metal-complexing ability of **4** has precluded the accurate elemental analysis.

3-Methyl-4-propionyl-7-methoxyindole (5). A mixture of **4** (0.86 g, 3.3 mmol) and $CuCrO_4$ (0.4 g) in quinoline (20 mL) was heated at 200 °C for 3 h. After removal of the remaining solids by filtration, the filtrate was extracted with ether, washed with 1 N HCl, and dried over $MgSO_4$. Evaporation of the solvent gave pale brown solids from which **5** was isolated in a 59% yield by flash column chromatography (SiO_2, $CHCl_3$): mp 138−140 °C; IR (KBr) 3300 (NH), 1652 cm^{-1} (C=O); ^{1}H NMR ($CDCl_3$) δ 1.26 (3 H, t, J = 7.3 Hz, CH_2CH_3), 2.35 (3 H, d, J = 1.1 Hz, 3-CH_3), 3.02 (2 H, q, J = 7.3 Hz, CH_2CH_3), 3.99 (3 H, s, 7-OCH_3), 6.59 (1 H, d, J = 7.8 Hz, 6-H), 7.03 (1 H, br s, 2-H), 7.47 (1 H, d, J = 7.8 Hz, 5-H), 8.32 (1 H, br s, NH); MS (EI) m/z 217 (M^+). Anal. Calcd for $C_{13}H_{15}NO_2$: C, 71.85; H, 6.96; N, 6.45. Found: C, 71.57; H, 6.93; N, 6.32.

3-Methyl-4-(3′-methylindol-2′-yl)-7-methoxyindole (6). An ethanol (20 mL) solution of **5** (370 mg, 1.7 mmol) and phenylhydrazine hydrochloride (370 mg, 2.6 mmol) containing concentrated H_2SO_4 (1 mL) was stirred at the refluxing temperature for 8 h. The reaction mixture was diluted with water, extracted with CH_2Cl_2, and dried over $MgSO_4$. Removal of the solvent gave yellow solids from which **6** was isolated as a white solid in a 71% yield by flash column chromatography (SiO_2, $CHCl_3$): mp 227−229 °C; IR (KBr) 3420 cm^{-1} (NH); ^{1}H NMR ($CDCl_3$) δ 1.87 (3 H, d, J = 1.4 Hz, 3-CH_3), 2.25 (3 H, s, 3′-CH_3), 4.02 (3 H, s, 7-OCH_3), 6.70 (1 H, d, J = 7.8 Hz, 6-H), 6.97 (1 H, m, 2-H), 7.03 (1 H, d, J = 7.8 Hz, 5-H), 7.14−7.24 (2 H, m, 5′-H and 6′-H), 7.36 (1 H, m, 7′-H), 7.62 (1 H, m, 4′-H), 7.96 (1 H, br, 1′-NH), 8.24 (1 H, br, 1-NH); MS (EI) m/z 290 (M^+). Anal. Calcd for $C_{19}H_{18}N_2O$: C, 78.58; H, 6.25; N, 9.65. Found: C, 78.26; H, 6.14; N, 9.46.

3-Methyl-4-(3′-methylindol-2′-yl)-7-hydroxyindole (7). A CH_3CN (10 mL) solution of **6** (220 mg, 0.78 mmol) and trimethylsilyl iodide (1.2 mL, 8.4 mmol) was stirred at the refluxing temperature for 8 h. The reaction mixture was then extracted with CH_2Cl_2, and the organic layer was washed with aqueous $Na_2S_2O_3$ and dried over $MgSO_4$. Evaporation of the solvent gave a crude product that was purified by flash column chroamtography (SiO_2, AcOEt/$CHCl_3$ = 1/9) (93% yield): mp 99−101 °C; IR (KBr) 3424 (NH), 3200−3550 cm^{-1} (OH); ^{1}H NMR ($CDCl_3$) δ 1.84 (3 H, d, J = 0.54 Hz, 3-CH_3), 2.22 (3 H, s, 3′-CH_3), 6.59 (1 H, d, J = 7.6 Hz, 6-H), 6.92 (1 H, d, J = 7.6 Hz, 5-H), 6.97 (1 H, br s, 2-H), 7.12−7.23 (2 H, m, 5′-H and 6′-H), 7.34 (1 H, m, 7′-H), 7.60 (1 H, m, 4′-H), 7.94 (1 H, br, 1′-NH), 8.24 (1 H, br, 1-NH); MS (EI) m/z 276 (M^+); HRMS m/z 276.1277 (M^+) calcd for $C_{18}H_{16}N_2O$ 276.1263.

3-Methyl-4-(3′-methylindol-2′-yl)indole-6,7-dione (1). To a CH_3CN solution of **7** (180 mg, 0.65 mmol) was added Fremy's salt (700 mg, 2.6 mmol) in H_2O containing 2.6 mmol of KH_2PO_4. The mixture was stirred at room temperature for 12 h and then extracted with CH_2Cl_2. After the extract was dried over $MgSO_4$, evaporation of the solvent gave a dark brown residue from which quinone **1** was isolated in a 57% yield by flash column chromatography (SiO_2, AcOEt): mp >300 °C; IR (KBr) 3412 (NH), 1628 cm^{-1} (C=O); ^{1}H NMR (DMSO-d_6) δ 1.53 (3 H, s, 3-CH_3), 2.31 (3 H, s, 3′-CH_3), 5.86 (1 H, s, 5-H), 7.04 (1 H, t, J = 7.9 Hz, 5′-H), 7.15 (1 H, s, 2-H), 7.15 (1 H, t,

(7) Chistoserdov, A. Y.; Tsygankov, Y. D.; Lidstrom, M. E. *Biochem. Biophys. Res. Commun.* **1990**, *172*, 211.
(8) Preliminary results have been published: Itoh, S.; Ogino, M.; Komatsu, M.; Ohshiro, Y. *J. Am. Chem. Soc.* **1992**, *114*, 7294.
(9) Perrin, D. D.; Armarego, W. L. F.; Perrin, D. R. *Purification of Laboratory Chemicals*; Pergamon Press: Elmsford, NY, 1966.
(10) Osakai, T.; Nuno, T.; Yamamoto, Y.; Saito, A.; Senda, M. *Bunseki Kagaku* **1989**, *38*, 479.
(11) Kano, K.; Sugimoto, T.; Misaki, Y.; Enoki, T.; Hatakeyama, H.; Oka, H.; Hosotani, Y.; Yoshida, Z. *J. Phys. Chem.* **1994**, *98*, 252.
(12) The AM1 method: Dewar, M. J. S.; Zoebisch, E. G.; Healy, E. F.; Stewart, J. J. P. *J. Am. Chem. Soc.* **1985**, *107*, 3902.
(13) Blaikie, K. G.; Perkin, W. H. *J. Chem. Soc.* **1924**, *125*, 269.

Scheme 1

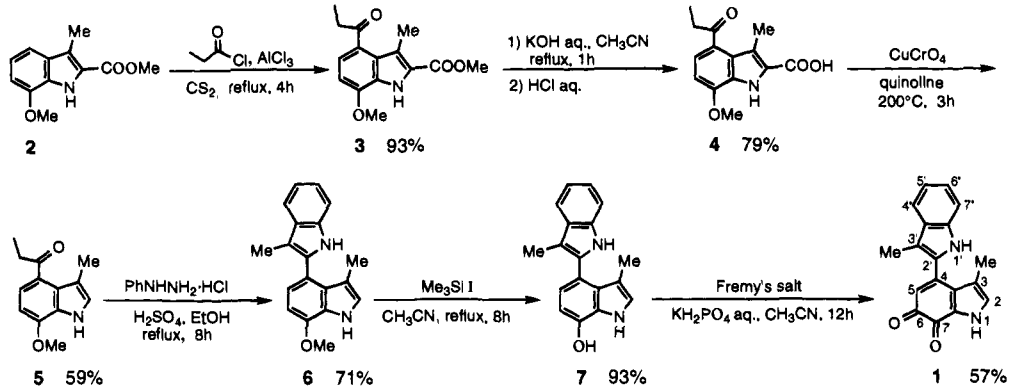

J = 7.9 Hz, 6′-H), 7.35 (1 H, d, J = 7.9 Hz, 7′-H), 7.56 (1 H, d, J = 7.9 Hz, 4′-H), 11.24 (1 H, br s, 1′-H), 12.74 (1 H, br s, 1-H); ^{13}C NMR (DMSO-d_6) 9.4 (CH_3), 10.7 (CH_3), 110.0, 111.6, 119.1, 119.3, 121.4, 122.8, 123.6, 127.4, 128.4, 128.7, 130.3, 130.7, 136.4, 144.2 (14 sp^2 carbons), 167.3 (d, $^2J_{CH}$ = 4.9 Hz, 6-C), 183.1 (s, 7-C) ppm; MS (EI) m/z 290 (M^+), 292 (M^+ + 2, characteristic peak for o-quinone compounds. Anal. Calcd for $C_{18}H_{14}O_2N_2$: C, 74.46; H, 4.86; N, 9.65. Found: C, 74.25; H, 4.86; N, 10.07.

Oxidation of 8 and 9 with Fremy's Salt. 6-Hydroxyskatole (**8**) was obtained by deprotection with iodotrimethylsilane of the methoxy group of 6-methoxyskatole, which was prepared by the reported procedure from m-anisidine.[14] 7-Hydroxyskatole (**9**) was obtained from **2** *via* ester hydrolysis, thermal decarboxylation, and deprotection of the methoxy group by the same procedure described above.

To a CH_3CN solution (12.7 mL) of **8** (30 mg, 0.20 mmol) was added Fremy's salt (364 mg, 0.82 mmol) in H_2O (13 mL) containing 0.82 mmol of KH_2PO_4 at 0 °C. The mixture was stirred at room temperature for 1.5 h and then extracted with ether. After the extract was dried over $MgSO_4$, evaporation of the solvent gave a dark brown residue from which o-quinone **10** and 2,6-dioxo derivative **11** were isolated in 7% and 63% yields, respectively, by flash column chromatography (SiO_2, n-hexane/AcOEt). Compound **10**: mp >300 °C; IR (KBr) 3180 (NH), 1632 cm^{-1} (C=O); ^{1}H NMR (DMSO-d_6) δ 2.07 (3 H, s, 3-CH_3), 5.85 (1 H, d, J = 9.7 Hz, 5-H), 7.09 (1 H, s, 2-H), 7.45 (1 H, d, J = 9.7 Hz, 4-H), 12.50 (1 H, br s, 1H, NH); ^{13}C NMR (DMSO-d_6) 9.0 (3-CH_3), 120.5, 122.8, 127.9, 128.7, 129.6, 137.5 (6 aromatic carbons), 166.6, 184.2 ppm (quinone carbonyl carbons); MS (EI) m/z 161 (M^+); HRMS m/z 161.0471 (M^+) calcd for $C_9H_7O_2N$ 161.0477. Compound **11**: mp >300 °C; IR (KBr) 3284 (NH), 1728, 1692, 1670, 1634 cm^{-1} (C=O and/or C=C); ^{1}H NMR ($CDCl_3$) δ 2.14 (3 H, s, 3-CH_3), 5.80 (1 H, s, 7-H), 6.20 (1 H, d, J = 9.9 Hz, 5-H), 7.13 (1 H, br s, NH), 7.21 (1 H, d, J = 9.9 Hz, 4-H); MS (EI) m/z 161 (M^+).

Oxidation of **9** with Fremy's salt was carried out in a similar manner. The flash column chromatographic treatment (SiO_2, n-hexane/AcOEt) of the resulting crude material gave o-quinone **10** in an 11% yield together with p-quinone **12** in a 64% yield: Compound **12**: mp 204–205 °C; IR (KBr) 3212 (NH), 1644 cm^{-1} (C=O); ^{1}H NMR (DMSO-d_6) δ 2.22 (3 H, s, 3-CH_3), 6.55 (1 H, d, J = 10.2 Hz, 5-H or 6-H), 6.61 (1 H, d, J = 10.2 Hz, 5-H or 6-H), 7.06 (1 H, s, 2-H), 12.50 (1 H, br s, NH); ^{13}C NMR (DMSO-d_6) 10.6 (3-CH_3), 120.6, 122.4, 125.2, 130.4, 136.4, 137.7 (6 aromatic carbons), 176.6, 184.2 ppm (quinone carbonyl carbons). MS (EI) m/z 161 (M^+). Anal. Calcd for $C_9H_7O_2N$: C, 67.07; H, 4.38; N, 8.69. Found: C, 67.02; H, 4.34; N, 8.49.

Coupling Reaction of o-Quinone 10 and Skatole. o-Quinone **10** (7.80 mg, 0.048 mmol) and skatole (6.35 mg, 0.048 mmol) were treated with $AlCl_3$ (33 mg, 0.25 mmol) in CH_3CN (5 mL) for 24 h under dark and a N_2 atmosphere. The mixture was poured onto ice and extracted with AcOEt. After it was dried over $MgSO_4$, model compound **1** was isolated by flash column chromatography (SiO_2, n-hexane/AcOEt) in an 18% yield.

3-Methyl-4-(3′-methylindol-2′-yl)-6,7-dihydroxyindole ($1H_2$). To a CH_3CN (10 mL) solution of **1** (15.22 mg, 0.0525 mmol) was added methylhydrazine (0.527 mmol, 10 equiv), and the reaction mixture was stirred for 1 h under anaerobic conditions (Ar). Removal of the solvent under reduced pressure gave a yellow residue from which $\mathbf{1H_2}$ was crystallized by adding n-hexane [11.1 mg (73% yield)]: mp >300 °C; IR (KBr) 3300–3500 cm^{-1} (OH and NH); ^{1}H NMR (DMSO-d_6) δ 1.68 (3 H, d, J = 0.5 Hz, 3-CH_3), 2.11 (3 H, s, 3′-CH_3), 6.55 (1 H, s, 5-H), 6.84 (1 H, br s, 2-H), 6.97–7.04 (2 H, m, 5′-H and 6′-H), 7.27 (1 H, d, J = 7.3 Hz), 7.45 (1 H, d, J = 6.8 Hz), 8.59 (2 H, br s, OH), 10.32 (1 H, br s, NH), 10.87 (1 H, br s, NH); MS (EI) m/z 292 (M^+).

Iminoquinone 13. Dry NH_3 gas was passed through a CH_3CN solution of **1** (2.0 mM) for 10 min, and the reaction mixture was stirred at room temperature for several hours. Removal of the solvent quantitatively gave an iminoquinone derivative as a brown solid: mp >300 °C; IR (KBr) 3212 (NH), 1642 and 1619 cm^{-1} (C=O and C=N); UV–vis (CH_3CN, λ_{max}) 228 (ϵ = 38 000 M^{-1} cm^{-1}), 282 (11 000), 376 nm (6200); ^{1}H NMR (DMSO-d_6) δ 1.49 (3 H, s, 3-CH_3), 2.27 (3 H, s, 3′-CH_3), 6.34 (1 H, s, 5-H), 7.03 (1 H, t, J = 7.7 Hz, 5′-H), 7.12 (1 H, t, J = 7.7 Hz, 6′-H), 7.20 (1 H, s, 2-H), 7.33 (1 H, d, J = 7.7 Hz, 7′-H), 7.54 (1 H, d, J = 7.7 Hz, 4′-H), 11.17 (1 H, br s, NH), 11.71 (1 H, br s, NH), 12.66 (1 H, br s, NH); MS (EI) m/z 289 (M^+); HRMS m/z 289.1223 (M^+) calcd for $C_{18}H_{15}N_3O$ 289.1217.

Results and Discussion

Synthesis. TTQ model compound **1** is designed to have exactly the same ring skeleton as the TTQ cofactor, but the two peptide chains at the 3- and 3′-position are displaced by simple methyl groups as shown in Scheme 1. Friedel–Crafts acylation on indole derivative **2** with propionyl chloride by the standard method gave the 4-acylated derivative **3** in a 93% yield. The position of the acylation in **3** was confirmed by ^{1}H NMR; a large NOE (18%) was detected on 6-H with irradiation at 7-OMe. When the Friedel–Crafts acylation was carried out on 7-methoxyskatole, a propionyl group was introduced predominantly at the 2-position. Indole derivative **3** was then converted into **5** by ester hydrolysis, followed by thermal decarboxylation using $CuCrO_4$ in quinoline at 200 °C. When the thermal decarboxylation was carried out at a higher temperature (240 °C) in glycerol, the deacylation occurred together with the decarboxylation to afford 7-methoxyskatole. The second indole ring was then constructed by Fischer indolization on **5** with phenylhydrazine hydrochloride in refluxing ethanol containing a small amount of H_2SO_4. Deprotection of the methoxy group of **6** by trimethylsilyl iodide gave 7-hydroxy derivative **7**, which was finally converted into the expected quinone **1** by oxidation with Fremy's salt in aqueous CH_3CN–KH_2PO_4.

It has been suggested that TTQ is formed *via posttranslational modification* of two tryptophan residues of the MADH subunit peptide chain and that one of the precursors is the 6,7-indolequinone derivative of the tryptophan that combines with another tryptophan residue existing near the 4-position of the quinone.[1] In this study, we have also tried to synthesize TTQ

(14) Nordlander, J. E.; Catalane, D. B.; Kotian, K. D.; Stevens, R. M.; Haky, J. E. *J. Org. Chem.* **1981**, *46*, 778.

model compound **1** by mimicking one of the speculated biosynthetic pathways that involves the coupling reaction between a 6,7-indolequinone derivative and an indole derivative itself.

The 6,7-indolequinone derivative of tryptophan might be produced from 6- or 7-hydroxytryptophan that could be derived *via* direct hydroxylation of the tryptophan residue. However, no regioselective hydroxylation at the 6- or 7-position of indoles has been reported so far.[15] In the Fenton and Udenfriend reactions, tryptophan is converted into many products unselectively.[16,17] Direct hydroxylation of the benzene ring of indole derivatives was reported to occur in the reaction with hydrogen peroxide in super acids, but the regioselectivity was also poor.[18] Since it has been suggested that a peroxidase-type enzyme is involved in the TTQ biosynthesis,[19] we have examined enzymatic oxygenation of a 3-substituted indole such as skatole using a horseradish peroxidase or chloroperoxidase system.[20] However, ring-opening and dimeric products were mainly obtained. Further studies are required to know how the 6- or 7-position of the indole ring is activated for an oxygenation reaction during the biosynthetic process of TTQ.

Thus, we have employed 6- and 7-hydroxyskatoles **8** and **9** as the model compounds of 6- and 7-hydroxytryptophans, respectively. Oxidation of 6-hydroxyskatole (**8**) with Fremy's salt by the standard procedure gave the expected *o*-quinone derivative **10** in a 7% yield (eq 2). Unexpectedly, a relatively large amount of 2,6-dioxo derivative **11** was also produced (63% yield). The same treatment on **9** gave *o*-quinone **10** together with *p*-quinone **12** in 11% and 64% yields, respectively (eq 3). The regioselectivities, 2,6- *vs* 6,7- and 4,7- *vs* 6,7-, may be determined by the electron spin density of the radical intermediates that are formed during the Fremy's salt oxidation.[21]

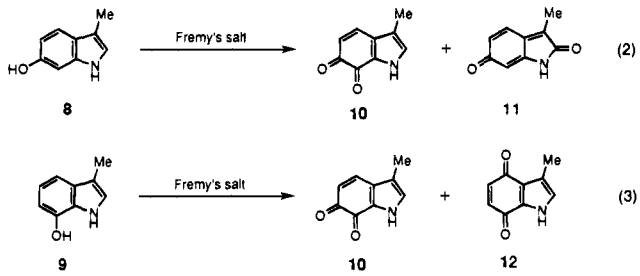

The coupling reaction between *o*-quinone **10** and skatole itself was then examined in CH_3CN at room temperature. No reaction takes place in the absence of any additive, but we have found that $AlCl_3$ works as a catalyst to afford the expected model compound **1** in an 18% isolated yield (eq 4). The primary product of the reaction may be the quinol form $\mathbf{1H_2}$ that can be readily oxidized by molecular oxygen to generate quinone **1** during the workup treatment. Although the detailed function of $AlCl_3$ is not clear at present, the $AlCl_3$ coordination to the quinone function may activate the 4-position of **10** toward the nucleophilic addition of skatole. The coordination of $AlCl_3$ may also occur with skatole at the 1-N position, resulting in an enhancement of the nucleophilicity at the 2-position of skatole.

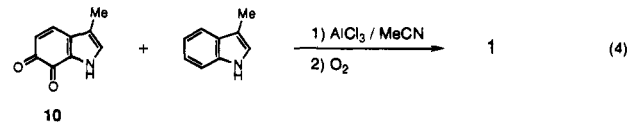

Thus, model compound **1** has also been synthesized successfully by mimicking one of the postulated biosynthetic routes to TTQ. The present results provide valuable insight into a possible biosynthetic route of TTQ as shown in Scheme 2, although the regioselective hydroxylation of 3-substituted indoles and the effective 6,7-indolequinone formation have not yet been achieved. The regioselective introduction of an oxy function into indoles by a chemical process is so difficult that there may be an unknown enzyme that catalyzes the hydroxylation of the 6- and/or 7-positions of tryptophan. Once the 6,7-indolequinone is formed, TTQ may be constructed spontaneously by means of acid–base catalysis in the enzyme active site (so-called self-catalysis).

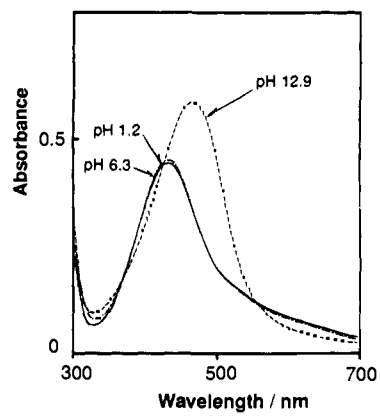

Figure 1. UV–vis spectra of **1** (5.0×10^{-5} M) in 0.1 M buffer solution containing 10% (v/v) DMSO at pH 1.2, 6.3, and 12.9.

Scheme 2

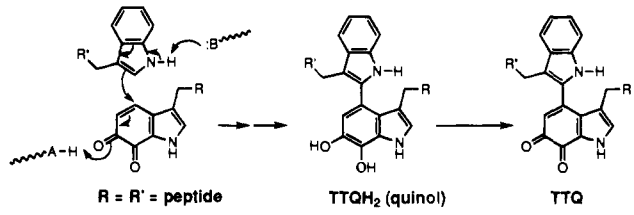

Spectroscopic Characterization. UV–vis spectra of compound **1** are examined under several pH conditions. Figure 1 shows the typical ones at pH 1.2, 6.3, and 12.9 in an aqueous buffer solution containing 10% DMSO. At a wide pH range from 1 to 9, the spectrum is practically unchanged (λ_{max} = 434 nm, $\epsilon = 9.2 \times 10^3$ M^{-1} cm^{-1}), but above pH 9, the absorbance at 434 nm decreases, accompanied by an increase in absorbance at 469 nm with isosbestic points at 361, 436, and 549 nm (λ_{max} = 469 nm, $\epsilon = 1.21 \times 10^4$ M^{-1} cm^{-1} at pH 12.9). The acid-dissociation constant (K_a) of **1** was then determined by monitoring the increase at 469 nm. The pH dependence of the absorbance in Figure 2 provides a best fit to a least-squares titration curve for a monobasic acid of pK_a = 10.6. The pK_a value indicates the dissociation of 1-NH (the pyrrole proton of the indolequinone) rather than that of 1′-NH since 3-methyl-

(15) Remers, W. A.; Spande, T. F. In *The Chemistry of Heterocyclic Compounds: Indoles, Part 3*; Houlihan, W. J., Ed.; John Wiley & Sons: New York, 1979; pp 9–11.

(16) Uchida, K.; Enomoto, N.; Itakura, K.; Kawakishi, S. *Arch. Biochem. Biophys.* **1990**, *279*, 14.

(17) Maskos, Z.; Rush, J. D.; Koppenol, W. H. *Arch. Biochem. Biophys.* **1992**, *296*, 514.

(18) Berrier, C.; Jacquesy, J.-C.; Jouannetaud, M.-P.; Renoux, A. *Tetrahedron Lett.* **1986**, *27*, 4565.

(19) Page, M. D.; Ferguson, S. J. *Eur. J. Biochem.* **1993**, *218*, 711.

(20) The enzymatic oxygenation of skatole was carried out in 0.1 M phosphate buffer solution (pH 6.6) containing 20% CH_3CN at 30 °C according to the reported procedure: Colonna, S.; Gaggero, N.; Carrea, G.; Pasta, P. *J. Chem. Soc., Chem. Commun.* **1992**, 357. The reaction mixture was analyzed by GC–MS and ^1H NMR.

(21) For details about the mechanism of Fremy's salt oxidation, see: Thomson, R. H. In *The Chemistry of the Quinonoid Compounds, Part 1*; Patai, S., Ed.; John Wiley & Sons: London, 1974; pp 111–161.

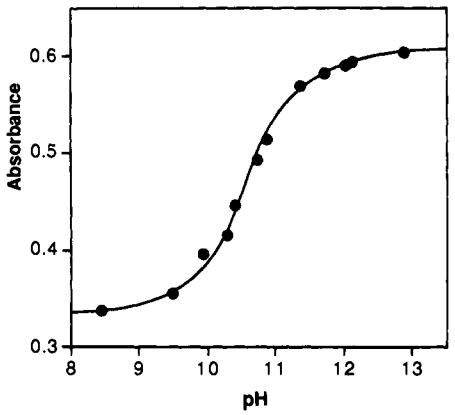

Figure 2. Spectroscopic determination of pK_a of **1** in 0.1 M buffer solution containing 10% (v/v) DMSO. Absorption at 469 nm is plotted against pH.

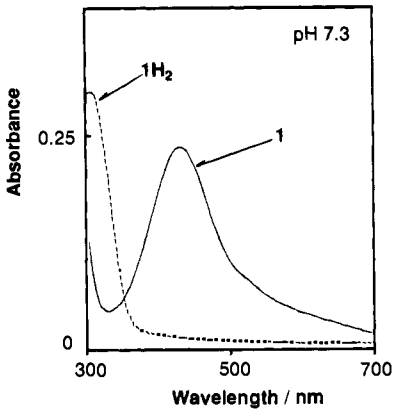

Figure 3. UV−vis spectra of **1** and **1H$_2$** (5.0×10^{-5} M) in CH_3CN. **1H$_2$** was generated *in situ* by the reduction of **1** with methylhydrazine (10 equiv).

4-phenylindole-6,7-quinone shows a similar pK_a at 10.7.[22] The ^{1}H NMR data of **1** also suggest that electron density of 1-NH is less than that of 1′-NH (Δ1.50 ppm downfield-shifted). No appreciable change in the spectrum has been observed during the measurements at each pH condition, indicating that there is no side reaction such as hydration of the quinone carbonyl group.

Compound **1** shows a similar spectral shape in CH_3CN (λ_{max} = 407 nm, $\epsilon = 1.07 \times 10^4$ M^{-1} cm^{-1}, with a broad shoulder at 500−650 nm) as compared with that in aqueous solution. The absorption maximum (λ_{max}) is shifted, however, toward a shorter wavelength by *ca.* 30 nm. It has been reported that $MADH_{ox}$ from bacterium W3A1 gives λ_{max} at 429 nm[23] and that from *Paracoccus denitrificans* gives λ_{max} at 440 nm[24] under neutral pH conditions. The difference in λ_{max} may reflect the microenvironmental difference in the enzyme active sites. Considering the blue shift of λ_{max} of **1** in changing the solvent from water to CH_3CN, it can be said that TTQ of the bacterium W3A1 enzyme exists in a more hydrophobic environment than that of *P. denitrificans* MADH. Reduction of **1** to **1H$_2$** by methylhydrazine[25] results in the complete disappearance of absorbance in the long wavelength region, accomapnied by a rise in absorbance at 306 nm ($\epsilon = 1.23 \times 10^4$ M^{-1} cm^{-1}) as shown in Figure 3. The spectrum of **1H$_2$** also resembles in shape that of $MADH_{red}$ (bacterium W3A1, λ_{max} = 331 nm and *P. denitrificans*, λ_{max} = 326 nm at pH 7.5). The resonance

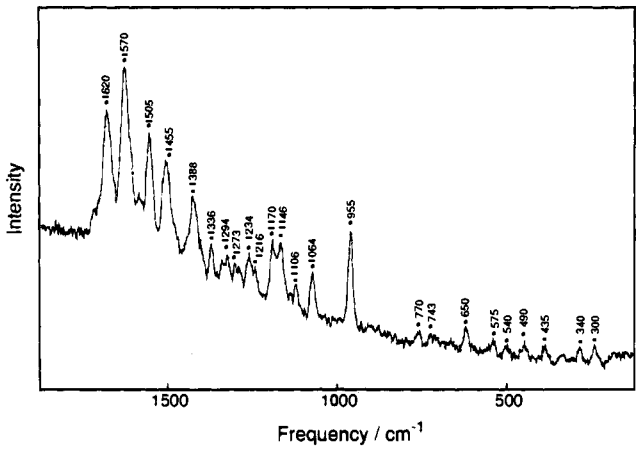

Figure 4. Resonance Raman spectrum of **1** obtained by using 457.9 nm excitation (100 mW) (KBr disk sample).

Raman spectrum of **1** is shown in Figure 4. There is also a good spectral similarity between the model compound and native TTQ in the enzyme active site.[4,26] For example, the C=O vibrational mode of **1** appears at 1620 cm^{-1}, which is essentially the same as that of MADHs: 1614 cm^{-1} for bacterium W3A1 MADH, 1625 cm^{-1} for *P. denitrificans* MADH, and 1625 cm^{-1} for newly found TTQ-containing enzyme AADH (aromatic amine dehydrogenase) from *Alcaligenes faecalis*.[27]

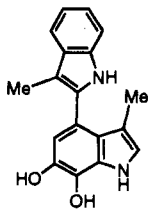

1H$_2$

The mass spectrum gives a strong peak of M + 2, which is a characteristic one for *o*-quinone compounds,[28] at 292 together with the parent peak at 290. A strong IR absorption of carbonyl stretching of the quinone moiety appears at 1628 cm^{-1}, which is lower by about 50 cm^{-1} than that of ordinary *o*-quinones.[29] This result may indicate that the conjugation between the *o*-quinone group and the indole ring and the double bond between 4-C and 5-C is relatively strong.[30] The ^{13}C NMR signals due to the quinone carbonyl carbons at the 6-C and 7-C positions appear at 167.3 and 183.1 ppm, respectively. The high-field signal due to 6-C as compared with that of normal quinones also indicates a relatively higher degree of conjugation, particularly at the 6-C carbonyl group. The ^{1}H NMR spectra in DMSO have fitted the TTQ structure as well. It is interesting

(22) Synthesis and characterization of other TTQ models including 3-methyl-4-phenylindole-6,7-quinone will be reported elsewhere.
(23) Kenney, W. C.; McIntire, W. *Biochemistry* **1983**, *22*, 3858.
(24) Husain, M.; Davidson, V. L. *Biochemistry* **1987**, *26*, 4139.
(25) Hydrazines are known to deactivate MADHs by forming hydrazone adducts (see refs 5b and 23), but compound **1** is cleanly reduced by methylhydrazine to the corresponding quinol *in vitro*. The reason for the difference between the enzymatic and non-enzmatic system is not clear now, but a microenvironmental effect such as general acid−base catalysis of the enzyme active site would affect the reaction pathway. In the case of coenzyme PQQ, pH of the reaction media has been revealed to alter the reaction pathway, redox reaction *vs* adduct formation: Mure, M.; Nii, K.; Itoh, S.; Ohshiro, Y. *Bull. Chem. Soc. Jpn.* **1990**, *63*, 417.
(26) McIntire, W. S.; Bates, J. L.; Brown, D. E.; Dooley, D. M. *Biochemistry* **1991**, *30*, 125.
(27) Govindaraj, S.; Eisenstein, E.; Jones, L. H.; Sanders-Loehr, J.; Chistoserdov, A. Y.; Davidson, V. L.; Edwards, S. L. *J. Bacteriol.* **1994**, *176*, 2922.
(28) Zeller, K.-P. In *The chemistry of the quinonoid compounds, Part 1*; Patai, S., Ed.; John Wiley & Sons: London, 1974; p 231.
(29) Berger, St.; Rieker, A. In *The chemistry of the quinonoid compounds, Part 1*; Patai, S., Ed.; John Wiley & Sons: London, 1974; p 193.
(30) Electronic effects of the C-4 substituent will be discussed in detail elsewhere (ref 22).

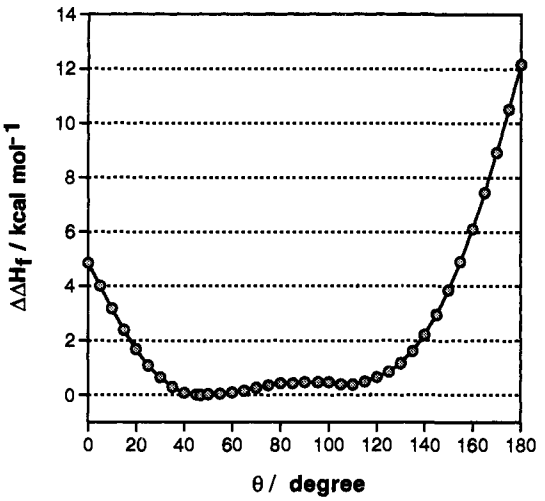

Figure 5. Plot of $\Delta\Delta H_f$ (ΔH_f values relative to that of the most stable conformation at $\theta = 46.9°$) of **1** *vs* the dihedral angle (θ) of the two indole rings defined by 5-C−4-C−2′-C−3′-C. Calculated by the AM1 method.

to note that the signal of 3-CH_3 (δ 1.53) appears at a higher magnetic field than that of 3′-CH_3 (δ 2.31). Such a high-field shift may be ascribed to the molecular geometry of the compound (*vide infra*).

Molecular Geometry. X-ray crystallographic investigation of MADHs from *P. denitrificans* and *Thiobacillus versutus* has revealed that the dihedral angle of the two indole rings of TTQ is about 42°.[2a] Molecular orbital calculations by the AM1 method indicated that the dihedral angle of the two indole rings, defined by 5-C−4-C−2′-C−3′-C, in the optimized structure of compound **1** is 46.9° and the distance between the protons of 3′-CH_3 and 5-H and that of 3′-CH_3 and 3-CH_3 are about 2.7 and 4.7 Å, respectively. Such a molecular geometry is also suggested by the observed NOE correlation for **1**; an NOE of approximately 20% was detected between 3′-CH_3 and 5-H in contrast with that of a small value (4%) between 3′-CH_3 and 3-CH_3. The upfield shift of the methyl group at the 3-position (*vide supra*) may be ascribed to the ring current effect by the second indole moiety that is located just above 3-CH_3. The dependence of ΔH_f (heat of formation) on the dihedral angle (θ) of the two indole rings was calculated by using the AM1 method. The change of ΔH_f values ($\Delta\Delta H_f$) relative to that of the most stable conformation ($\theta = 46.9°$) with θ is shown in Figure 5, which demonstrates that the difference in the heat of formation is within 1 kcal/mol at a dihedral angle from *ca.* 30° to 130° (Figure 5). It is interesting to note that the molecular geometry of TTQ in the enzyme active site is almost adjusted to that having the minimum steric energy of the molecule in spite of the existing steric restriction through space and/or through peptide bonding around the enzyme active site.

Electrochemistry. Figure 6 shows cyclic voltammograms of compound **1** obtained in various buffer solutions at a scan rate (ν) of 20 mV s^{-1}. Compound **1** gives a pair of cathodic and anodic waves ascribed to a two-electron redox reaction of the *o*-quinone moiety. The voltammograms obtained at $\nu <$ 100 mV s^{-1} exhibit totally reversible characteristics; the peak separations are practically independent of ν, and the peak currents are proportional to $\nu^{1/2}$. The effect of pH on the midpoint potential (formal redox potential, $E^{\circ\prime}$) of the reversible voltammograms is depicted in Figure 7 with closed circles. The $E^{\circ\prime}$ *vs* pH profile is composed of three straight lines with slopes of −60 mV/pH (pH < 10), −30 mV/pH (10 < pH < 10.5), and −60 mV/pH (pH > 11). It is well-known that the slope is given by $-2.303mRT/nF$ for a ne^-, mH^+ process (F is the Faraday constant and $-2.303RT/F$ is −60 mV at 25 °C). Since

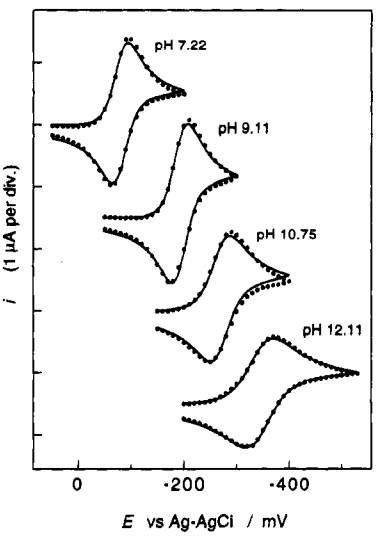

Figure 6. Background-corrected cyclic voltammograms of **1** at ν = 20 mV s^{-1} in aqueous buffers containing 20% (v/v) DMSO. The solid lines represent regression curves using digital simulation on the basis of the two-step one-electron redox reaction. Estimated values of $E^{\circ\prime}$ and $\Delta E^{\circ\prime}$ are given in Figure 7.

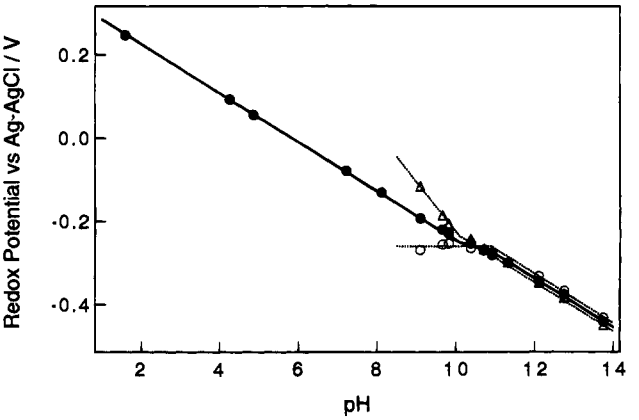

Figure 7. pH dependence of $E^{\circ\prime}$ (●), $E_1^{\circ\prime}$ (○), and $E_2^{\circ\prime}$ (△) of the **1**/**1H₂**, **1**/**1**$^{\bullet-}$, and **1**$^{\bullet-}$/**1H₂** couples, respectively. The $E^{\circ\prime}$ ($E^{\circ\prime} = E_1^{\circ\prime} + E_2^{\circ\prime}$) values were taken as the midpoint potentials of the reversible cyclic voltammograms. The values of $\Delta E^{\circ\prime}$ were estimated by digital simulation (see Figure 6 as examples).

the number of electrons involved in the electrode reactions in the present case is 2, the observed change in the slope with pH indicates that below pH 10, the electrode reaction is a $2e^-$, $2H^+$ process (eq 5), between pH 10 and 10.5, a $2e^-$, $1H^+$ process (eq 6), and above pH 11, a $2e^-$, $2H^+$ process (eq 7).

$$\mathbf{1} + 2e^- + 2H^+ \rightleftharpoons \mathbf{1H_2} \quad (5)$$

$$\mathbf{1} + 2e^- + H^+ \rightleftharpoons \mathbf{1H^-} \quad (6)$$

$$\mathbf{1}(-H^+) + 2e^- + 2H^+ \rightleftharpoons \mathbf{1H^-} \quad (7)$$

The inflection point appearing at pH 10.1 may correspond to the pK_a of **1H₂** due to the dissociation of the phenolic OH group since the acid dissociation of the pyrrole proton may be more difficult than the phenolic proton. Where the pH is higher than the pK_a of **1H₂**, the two-electron reduction of **1** is accompanied by the addition of one proton to yield **1H**$^-$ (eq 6). The other inflection point appearing at pH 10.9 may correspond to the pK_a of **1** due to the dissociation of 1-NH of **1**. The pK_a value of **1** thus determined electrochemically agrees well with that obtained independently by the spectral titration (10.6) in Figure 2. Where the pH of **1** is higher than pK_a, the

electrode reaction becomes a $2e^-$, $2H^+$ process, in which the deprotonated species [**1**($-\mathbf{H}^+$)] is reduced to **1H**$^-$ (eq 7). The interpolation affords the estimation of $E^{\circ\prime}$ *vs* Ag/AgCl at pH 7.0 as -0.090 V, which is converted to $E^{\circ\prime}$ *vs* NHE as 0.107 V. The $E^{\circ\prime}$ value is comparable to that of native MADHs from *P. denitrificans* and bacterium W3A1 ($E^{\circ\prime}$ *vs* NHE = 0.096 V at pH 7.5,[24,31] which would be corrected as 0.126 V at pH 7.0 by taking into account the $2e^-$, $2H^+$ process, and it is slightly more positive than those of other types of quinone cofactors, PQQ (pyrroloquinolinequinone, $E^{\circ\prime}$ *vs* NHE = 0.090[32] or 0.066 V[33] at pH 7.0) and topa quinone (2,4,5-trihydroxyphenylalanine quinone, $E^{\circ\prime}$ *vs* NHE = 0.079 V at pH 7.0;[34] topa hydantoin quinone, $E^{\circ\prime}$ *vs* NHE = 0.075 V at pH 7.0[35]).

Under neutral conditions, the voltammogram exhibits one-step two-electron characteristics with a peak separation of 30 mV. However, the reversible voltammogram is broadened at higher pH, and the peak separation reaches up to 50 mV at pH 12. Such a voltammetric behavior indicates that the two-electron reduction process is composed of overlapped two-step one-electron transfer processes that involve the generation of a semiquinone radical anion intermediate (**1**$^{\bullet-}$). For further characterization of the redox reaction, the first and second one-electron redox potentials of the **1**/**1**$^{\bullet-}$ and **1**$^{\bullet-}$/**1H**$_2$ couples ($E_1^{\circ\prime}$ and $E_2^{\circ\prime}$) are very important parameters. In this work, the differences between $E_1^{\circ\prime}$ and $E_2^{\circ\prime}$ ($\Delta E^{\circ\prime} = E_1^{\circ\prime} - E_2^{\circ\prime}$) were estimated by adjusting them to give the best fit to the voltammograms based on the digital simulation and nonlinear curve fitting,[11] which leads to the separate evaluation of $E_1^{\circ\prime}$ and $E_2^{\circ\prime}$ using the relation $E^{\circ\prime} = E_1^{\circ\prime} + E_2^{\circ\prime}$. The solid lines in Figure 6 show some results of the regression. The standard deviations of the $\Delta E^{\circ\prime}$ estimation were in a range of 2−4 mV at pH >9.5. However, the estimation error increased at lower pH because $\Delta E^{\circ\prime}$ becomes sufficiently negative, resulting in the characteristics of a one-step two-electron transfer. Reliable values of $E_1^{\circ\prime}$ and $E_2^{\circ\prime}$ are plotted against pH in Figure 7. The $E_1^{\circ\prime}$ (open circle) *vs* pH profile shows two straight lines with slopes of 0 mV/pH (pH < 11) for a $1e^-$ process (eq 8) and -60 mV/pH (pH > 11) for a $1e^-$, $1H^+$ process (eq 9). The inflection point at pH 10.9 corresponds to pK_a of **1**. On the other hand, the $E_2^{\circ\prime}$ (open triangle) *vs* pH profile shows two straight lines with slopes of -120 mV/pH (pH < 10) for a $1e^-$, $2H^+$ process (eq 10) and -60 mV/pH (pH > 10) for a $1e^-$, $1H^+$ process (eq 11) with an inflection point at pH 10.1, which corresponds to pK_a of **1H**$_2$.

$$\mathbf{1} + e^- \rightleftharpoons \mathbf{1}^{\bullet-} \quad (8)$$

$$\mathbf{1}(-\mathbf{H}^+) + e^- + H^+ \rightleftharpoons \mathbf{1}^{\bullet-} \quad (9)$$

$$\mathbf{1}^{\bullet-} + e^- + 2H^+ \rightleftharpoons \mathbf{1H_2} \quad (10)$$

$$\mathbf{1}^{\bullet-} + e^- + H^+ \rightleftharpoons \mathbf{1H}^- \quad (11)$$

These results indicate that the radical intermediate exists as an anion **1**$^{\bullet-}$ at pH > *ca.* 8. The pK_a of **1H**$^{\bullet}$ would be less than 6, as is the case for other typical quinones.[36] The radical anion **1**$^{\bullet-}$ is stabilized by the comproportionation reaction at the higher pH region. The comproportional constant (K_c) is evaluated to be 2.2 over a pH range of 12−14 according to the well-known relation $K_c = \exp(\Delta E^{\circ\prime}/RT)$ with $\Delta E^{\circ\prime} = E_2^{\circ\prime} - E_1^{\circ\prime}$. Bacterial MADH is known to accept two electrons from methylamine and to donate them sequentially to the one-electron acceptor amicyanin.[3,37] Thus, the characteristics of the two-step electron transfer of the TTQ cofactor seem to be essential for the enzymatic function.

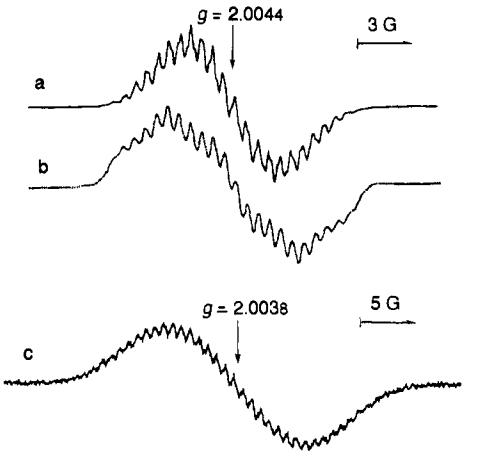

Figure 8. ESR spectra of (a) **1**$^{\bullet-}$ generated by half-reduction of **1** with $NaBH_4$ in methanol, (b) computer simulation spectra of **1**$^{\bullet-}$, and (c) the radical anion species derived from **13** by half-reduction of **1** with $NaBH_4$ in 2.0 M ammoniacal buffer containing 30% (v/v) DMSO at pH 9.5. Field modulation width was (a) 40 mG and (c) 400 mG at 100 kHz.

The generation of the semiquinone radical anion intermediate **1**$^{\bullet-}$ during the redox reaction has been supported by EPR measurements. The semiquinone radical anion was spontaneously generated from **1** under aqueous alkaline conditions or by half-reduction of **1** with $NaBH_4$ in slightly alkaline methanol. Figure 8a shows an observed spectrum obtained under such experimental conditions. The *g* value has been determined as 2.0044 ± 0.0002, which is within a range of those of ordinary semiquinone radical anions (2.0040−2.0050),[38,39] indicating the contribution of spin−orbit coupling due to electron spin at the oxygen nuclei. The resolution of the hyperfine structure has not been improved at a low-field modulation down to 40 mG.[40] Such a limited resolution may be attributed to a nonrigid conformation of **1**$^{\bullet-}$ in solution with a variation of the dihedral angle of the two indole rings (*vide supra*). Although the limited resolution has precluded the complete simulation, the hyperfine structures are reproduced well by the computer simulation with the hyperfine splitting (hfs) values of four nonequivalent protons (2.6, 1.8, 1.2, and 0.6 G), one set of methyl protons (0.5 G), and two nonequivalent nitrogen atoms (2.4 and 0.7 G) as shown in Figure 8b. The semiquinone radical anion **1**$^{\bullet-}$ contains eight nonequivalent protons (1-H, 2-H, 5-H, 1′-H, 4′-H, 5′-H, 6′-H, and 7′-H), two methyl protons (3-CH_3 and 3′-CH_3), and two nonequivalent nitrogen atoms (1-N and 1′-N). The AM1 calculation of **1**$^{\bullet-}$ indicates that there is essentially no spin density on the benzene ring (4′-C, 5′-C, 6′-C, and 7′-C) and that the spin density at the 3-C position is much smaller than

(31) Burrows, A. L.; Hill, H. A. O.; Leese, T. A.; McIntire, W. S.; Nakayama, H.; Sanghera, G. S. *Eur. J. Biochem.* **1991**, *199*, 73.
(32) Duine, J. A.; Frank Jzn., J.; Verwiel, P. E. J. *Eur. J. Biochem.* **1981**, *118*, 395.
(33) (a) Kano, K.; Mori, K.; Uno, B.; Kubota, T.; Ikeda, T.; Senda, M. *Bioelectrochem. Bioenerg.* **1990**, *23*, 227. (b) *Ibid.* **1990**, *24*, 193.
(34) Kano, K.; Mori, T.; Uno, B.; Goto, M.; Ikeda, T. *Biochim. Biophys. Acta* **1993**, *1157*, 324.
(35) Mure, M.; Klinman, J. P. *J. Am. Chem. Soc.* **1993**, *115*, 7117.
(36) Fukuzumi, S.; Ishikawa, K.; Hironaka, K.; Tanaka, T. *J. Chem. Soc., Perkin Trans. 2* **1987**, 751.
(37) (a) Tobari, J.; Harada, Y. *Biochem. Biophys. Res. Commun.* **1981**, *101*, 502. (b) Husain, M.; Davidson, V. L. *J. Biol. Chem.* **1985**, *260*, 14626. (c) Husain, M.; Davidson, V. L.; Smith, A. J. *Biochemistry* **1986**, *25*, 2431. (d) Gray, K. A.; Knaff, D. B.; Husain, M.; Davidson, V. L. *FEBS Lett.* **1986**, *207*, 239.
(38) Swarz, H. M.; Bolron, J. R.; Borg, D. C. *Biological Application of Electron Spin Resonance*; John Wiley & Sons: New York, 1972; p 24.
(39) Fukuzumi, S.; Nishizawa, N.; Tanaka, T. *J. Org. Chem.* **1984**, *49*, 3571.
(40) A similar spectrum was obtained under aqueous alkaline conditions, but the resolution was worse.

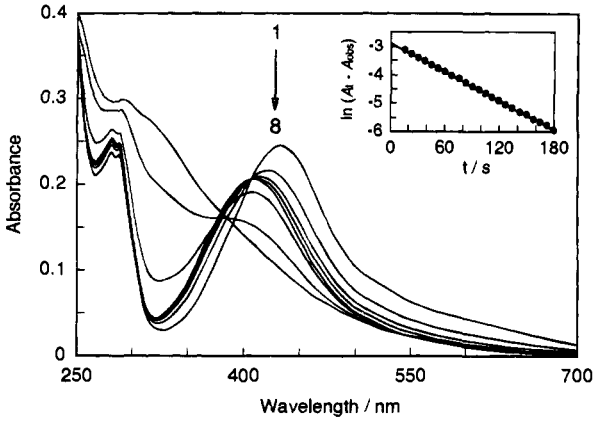

Figure 9. Time-dependent absorption spectra of **1** (2.0×10^{-5} M) in 1.0 M ammoniacal buffer containing 30% (v/v) DMSO at pH 9.5. The time after the addition of **1** into the buffer is (1) 0 s (in the absence of ammonia), (2) 45 s, (3) 90 s, (4) 135 s, (5) 5 min, (6) 2 h, (7) 10 h, and (8) 21.5 h. The spectrum change during 4−10 min was negligible (pseudo-equilibrated state). The inset represents plots for kinetic analysis during the shorter time window at 430 nm (see text for details).

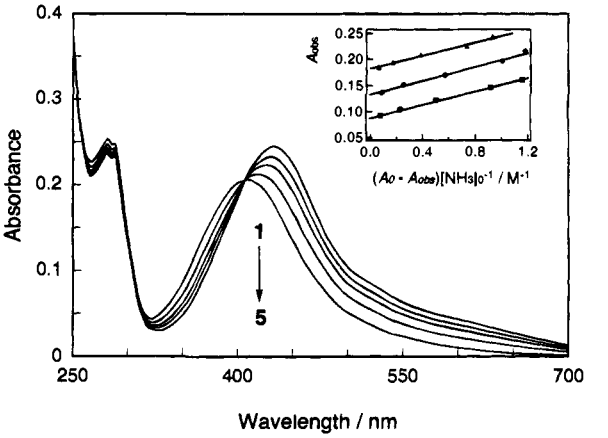

Figure 10. Ammonia concentration dependence of absorption spectra of the pseudo-equilibrated state of **1** (2.0×10^{-5} M) at pH 9.5 (30% (v/v) DMSO). $[NH_3]_0$: (1) 0 M, (2) 0.01 M, (3) 0.03 M, (4) 0.1 M, and (5) 1.0 M. The inset represents plots for equilibrium analysis at 430 (▲), 450 (●) and 470 (■) nm (see text for details).

that at the 3′-C position, agreeing with the observed hfs values.[41] Thus, the hfs values of 0.5 and 0.7 G may be assigned to those of the 3′-CH protons and 1′-N nitrogen, respectively. The spin delocalization on the 3′-C and 1′-N nuclei indicates partial π-conjugation with the second indole moiety. On the basis of the recent X-ray study on MADH/amicyanin/cytochrome c_{551i} ternary complex, it has been proposed that the electrons located on the quinoid cofactor are transferred to amicyanin through the second indole moiety.[3] Such an electron transfer would require a transient decrease in the dihedral angle in the semiquinone radical state (as well as in the fully reduced state).[42] The present EPR results on $\mathbf{1}^{\bullet-}$ seem to support the proposal in part.

Iminoquinone. It has been reported that ammonia has an influence on the activity of MADHs as in the case of other quinoproteins.[4,23,43] Thus, it seems of interest to study the interaction between **1** and ammonia. Figure 9 shows time-dependent spectral change upon spiking a 10 μL aliquot of the stock solution of **1** into 3.0 mL of 1.0 M ammoniacal buffer (pH 9.5). We have found that compound **1** reacts with ammonia to cause a blue shift in the longest wavelength absorption band with an isosbestic point at 408 nm (lines 1−5 in Figure 9). A pseudo-steady state in the spectrum (line 5) was attained in 3−10 min after the addition of **1**, depending on the total ammonia concentration ($[NH_3]_0$). The pseudo-steady state is followed by a very slow reaction, in which the absorption band around 400 nm disappears to give an isosbestic point at 380 nm (lines 6−8).[44] Such a spectral change can be ascribed to the reaction with free NH_3 (not NH_4^+) because no spectral change has occurred at pH 6.0, where practically all of ammoniacal components exist as NH_4^+.

The rate constant of the first phase reaction is much larger than that of the second one (*vide infra*), which allows us to see a pseudo-steady state of the first reaction. Figure 10 shows the effect of $[NH_3]_0$ on the absorption spectra at the pseudo-steady state. The existence of the identical isosbestic point at 408 nm is indicative of a thermodynamically reversible 1:1 complex formation between **1** and NH_3 for the first phase reaction. This behavior is similar to that observed in the reaction of PQQ with NH_3, in which 5-imino-PQQ is generated.[45−47] Thus, the product may be assigned as an iminoquinone derivative **13** (eq 12). In fact, the product **13** has been successfully isolated in the preparative-scale reaction of **1** and NH_3 gas in CH_3CN. Although satisfactory analytical data supporting the iminoquinone structure were obtained, the precise position of the nucleophilic addition has not been established (6-C or 7-C) at present.[48]

$$\mathbf{1} + NH_3 \underset{k_b}{\overset{k_f}{\rightleftharpoons}} \mathbf{13} + H_2O \qquad (12)$$

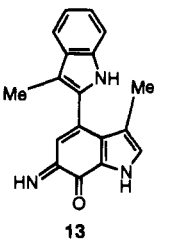

13

The dependence of the observed absorbance (A_{obs}) at the pseudo-equilibrated state on $[NH_3]_0$ was analyzed at a given wavelength to determine the apparent association constant ($K_{1,app} = [\mathbf{13}]/[\mathbf{1}][NH_3]_0$) by using eq 13,

$$A_{obs} = (A_o - A_{obs})/K_{1,app}[NH_3]_0 + A_{com} \qquad (13)$$

where A_o and A_{com} are the absorbances of **1** and **13**, respectively. Plots of A_{obs} against $(A_o - A_{obs})/[NH_3]_0$ at 430, 450, and 470 nm all gave a straight line as shown in the inset of Figure 10. Slopes of the three lines are essentially identical with one

(41) The spin densities were calculated with the RHF formalism since the calculation with the UHF formalism resulted in a significant spin-mixing, which has precluded the detailed comparison between the calculated spin densities and the observed hfs values.

(42) Brooks and Davidson proposed the same idea to account for the large reorganization energy that is associated with the electron transfer reaction from MADH to amicyanin: Brooks, H. B.; Davidson, V. L. *Biochemistry* **1994**, *33*, 5696.

(43) McIntire, W. S. *J. Biol. Chem.* **1987**, *262*, 11012.

(44) This isosbestic point was observed over a few hours. The absorption band around 400 nm was found to decrease obeying the pseudo-first-order kinetics. Kédzy−Swinbourne plots (Cornish-Bowden, A. *Principle of Enzyme Kinetics*; Butterworths: London, 1976; pp 7−9) gave a straight line, giving a rate constant of 3.3×10^{-5} s^{-1} at $[NH_3]_0 = 1.0$ M. However, the isosbestic point gradually moved toward a shorter wavelength afterward. Therefore, the second phase product might suffer some other reaction. The reaction product was found to be electrochemically inactive.

(45) Dekker, R. H.; Duine, J. A.; Frank Jzn., J.; Viewiel, P. E. J.; Westerling, J. *Eur. J. Biochem.* **1982**, *125*, 69.

(46) (a) Mure, M.; Itoh, S.; Ohshiro, Y. *Tetrahedron Lett.* **1989**, *30*, 6875. (b) Itoh, S.; Mure. M.; Ogino, M.; Ohshiro, Y. *J. Org. Chem.* **1991**, *56*, 6857.

(47) Kano, K.; Mori, K.; Uno, B.; Goto, M. *J. Electroanal. Chem. Interfacial Electrochem.* **1990**, *293*, 177.

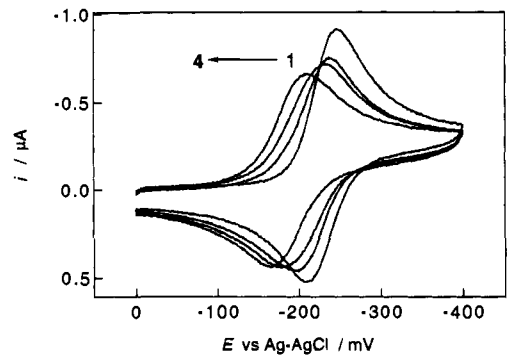

Figure 11. Ammonia concentration dependence on cyclic voltammograms of the pseudo-equilibrated state of **1** (6.0×10^{-5} M) at pH 9.5 (30% (v/v) DMSO). $[NH_3]_0$: (1) 0 M, (2) 0.03 M, (3) 0.1 M, and (4) 1.0 M. The voltammograms were recorded at $v = 10$ mV s^{-1}.

another, yielding the $K_{1,app}$ value of 15.5 ± 0.6 M^{-1} at pH 9.5. Assuming pK_a of NH_4^+ as 9.25 in this medium, the true dissociation constant ($K_1 = [\mathbf{13}]/[\mathbf{1}][NH_3] = k_f/k_b = K_{1,app}[(K_a + [H^+])/K_a]$) is evaluated as 24 M^{-1}. The K_1 value is 3-fold smaller than that of PQQ in aqueous solution (69 M^{-1} as K_1 at 25 °C[45]). The kinetics of formation of **13** were also examined by monitoring the time course of the absorbance (A_t) at 430 nm and at various $[NH_3]_0$. The decrease in A_t obeys the pseudo-first-order kinetics; plots of $\log(A_t - A_{obs})$ against the time (t) gave a straight line at each $[NH_3]_0$. An example is given in the inset of Figure 9. The linear plots allow for the estimation of the rate constants ($k_f[NH_3] + k_b$) by using eq 14. The k_f and k_b

$$\ln[(A_o - A_{obs})/(A_t - A_{obs})] = (k_f[NH_3] + k_b)t \quad (14)$$

values are determined as 2.8×10^{-2} M^{-1} s^{-1} and 1.2×10^{-3} s^{-1}, respectively, from the slope and intercept of the plot of ($k_f[NH_3] + k_b$) vs $[NH_3]_0$ by taking account for K_a of NH_4^+.

Iminoquinone **13** has a quinonoid structure and thus is expected to show characteristics of a reversible electron transfer. This is confirmed by the cyclic voltammetry measurements as shown in Figure 11, where the voltammograms were recorded after the pseudoequilibrium between **1** and **13** was reached at various $[NH_3]_0$ and at pH 9.5. With an increase in $[NH_3]_0$, the peak potential shifts in the positive potential direction and is accompanied by the broadening of the peak separation while retaining the reversibility. Since most of **1** (94% as calculated using the above $K_{1,app}$ value) is converted into **13** at $[NH_3]_0$ = 1.0 M (pH 9.5), the reversible voltammetric waves may be ascribed to the two-electron redox process of **13**. The voltammogram at $[NH_3]_0$ = 1.0 M shows the midpoint potential of −0.187 V, which is 41 mV higher than that of **1** in the absence of NH_3 at the same pH. A similar positive shift of the redox potential upon the iminoquinone formation has been reported for PQQ[45,47] and topa hydantoin quinone.[35] The two-electron reduction process is also composed of overlapped two-step one-electron transfer processes that involve the generation of an iminosemiquinone radical anion intermediate (**13**$^{\bullet-}$). Digital simulation analysis of the voltammogram (*vide supra*) has yielded the comproportionation constant $K_c = 0.7$, while the K_c value of **1** is estimated to be 0.02 at the same pH. Thus, iminosemiquinone radical anion **13**$^{\bullet-}$ is more stable than **1**$^{\bullet-}$, as is the case for imino-PQQ.[47] Such a difference in the redox properties between **1** and **13** may provide an interesting insight into the role of ammonia in the MADH activity, provided that TTQ cofactor in MADH is converted to the corresponding iminoquinone form in the presence of ammonia. It has been reported that the W3A1 enzyme is activated by ammonia at low concentrations.[43]

The generation of a radical anion intermediate has also been examined by EPR measurements. The radical anion was generated by half-reduction of **1** with $NaBH_4$ in the presence of NH_3 (pH 9.5) when a strong EPR signal was detected as shown in Figure 8c. It should be noted that the EPR signal of **1**$^{\bullet-}$ under the same experimental conditions was too weak to be observed clearly, as expected from the small K_c values of **1** as compared with **13** (*vide supra*). Although the poor resolution of the EPR spectrum (Figure 8c) has precluded the determination of the hfs values and unequivocal assignment of the observed radical species, some characteristics of the EPR signals are worthy of note. First, the total spectral width of the radical species derived from **13** is significantly broadened up to *ca.* 32 G as compared with that of **1**$^{\bullet-}$ (*ca.* 15 G). Such an increase in the spectrum width is certainly ascribed to the additional coupling caused by the NH group incorporated into **13**. Second, the g value is 2.0038 ± 0.0002, which is smaller than that of **1**$^{\bullet-}$, reflecting the spin localization on the nitrogen atoms rather than on the oxygen atom as observed in the case of flavosemiquinones (2.0030−2.0040).[38]

Concluding Remarks

TTQ model compound **1** has been synthesized in good yields according to Scheme 1. Another simple route mimicking one of the speculated biosynthetic pathways has also been investigated. Successful synthesis of **1** *via* the latter procedure suggests a possibility of the biosynthetic pathway illustrated in Scheme 2. Strong resemblances in several spectroscopic characteristics and redox potentials between **1** and TTQ cofactor have demonstrated the value of the model compound to deduce the *structural information* of the MADH active center. The direct detection of the semiquinone radical anion by EPR has also provided valuable information on structure as well as redox behavior. Examination of the iminoquinone formation and its redox property may provide an important insight into the action of ammonia for the MADH activity. In the preliminary study on the reaction of **1** and amines, we have found that **1** can act as a very efficient turnover catalyst for the aerobic oxidation of benzylamine,[8] indicating that **1** is also a good *functional model* of MADH. Further mechanistic details and structure−reactivity relationships of the amine oxidation reaction are now in progress.[22]

Acknowledgment. The present study was financially supported in part by a Grant-in-Aid for Scientific Research (No. 03403016) and for Priority Area (No. 05235227 and 05235103) from the Ministry of Education, Science, and Culture of Japan. We thank Professor Akira Nakamura and Dr. Norikazu Ueyama of Osaka University for assistance in obtaining the resonance Raman spectrum and the Instrumental Analysis Center, Faculty of Engineering, Osaka University, for the measurement of mass spectra on a JEOL JMS-DX303 spectrometer.

JA9428164

(48) The X-ray structure of the MADH active site revealed that there is a pocket for substrate binding near the carbonyl group at the 6-position, indicating the addition position of the substrate is 6-C: Huizinga, E. G.; van Zanten, B. A. M.; Duine, J. A.; Jongejan, J. A.; Huitema, F.; Wilson, K. S.; Hol, W. G. J. *Biochemistry* **1992**, *31*, 9789 and ref 2. However, one should be careful to conclude the addition position without any direct evidence. In the case of PQQ, both 4-C and 5-C methanol adducts were isolated depending on the reaction conditions: Itoh, S.; Ogino, M.; Fukui, Y.; Murao, H.; Komatsu, M.; Ohshiro, Y.; Inoue, T.; Kai, Y.; Kasai, N. *J. Am. Chem. Soc.* **1993**, *115*, 9960.